



MECHANICAL PROPERTIES OF MONOCRYSTALLINE C11_b MoSi₂ WITH SMALL ALUMINUM ADDITIONS

P. Peralta, S.A. Maloy, F. Chu, J.J. Petrovic and T.E. Mitchell
Materials Science and Technology Division, Los Alamos National Laboratory,
Los Alamos, NM 87545

(Received June 11, 1997)

(Accepted July 16, 1997)

1. Introduction

Molybdenum disilicide (MoSi₂) is a promising material for high temperature structural applications due to its high oxidation resistance, low density compared to nickel superalloys and high specific stiffness [1]. These advantages are hindered by its poor low temperature fracture toughness, which in polycrystals deteriorates with increasing temperature due to the presence of glassy silica in the grain boundaries that produces intergranular fracture [1]. One approach to avoid this is to reduce or modify the silica by alloying MoSi₂ with elements with higher affinity for oxygen than that of Si, such as Al, Ti, Zr and Y, for example [2-4]. Among these, Al offers the additional incentive of having some solid solubility in MoSi₂, which in turn has been suggested as a means to give a more "metallic character" to this silicide [5]. A slight decrease in the Vickers hardness of polycrystalline C11_b Mo(Si,Al)₂ (small Al additions) has been reported [4], whereas the results of Inui *et al.* [6] on the properties of C40 Mo(Si,Al)₂ single crystals (more than 10 at%Al [6]) indicate that large Al additions decrease the ductility and fracture toughness as compared with pure MoSi₂. Given that the effects of small Al additions on the mechanical properties of single crystals have not yet been explored, a study of the Vickers hardness for different crystallographic planes and directions has been carried out in monocrystalline Mo(Si,Al)₂ with the tetragonal C11_b structure at room temperature and the results compared to measurements carried out in pure MoSi₂ single crystals.

2. Experimental

A rod, 9 mm in diameter and 100 mm long, with nominal composition MoSi_{1.94}Al_{0.06} was prepared by arc melting high purity Mo, Si and Al. This rod was used to grow a single crystal using the Optical Floating Zone (OFZ) technique under argon flow at a maximum growth rate of 35 mm/hr. Single crystals of pure MoSi₂ were prepared in a similar fashion. Rectangular parallelepipeds with dimensions 5 × 5 × 10 mm³ for hardness testing were cut from the as grown single crystals with the edges along the [110], [$\bar{1}$ 10], and [001] directions as determined by the back-reflection Laue method. The samples were polished with SiC paper to 3 μm and finished with 1 μm diamond paste. Indentation tests were

carried out in a microhardness tester using a standard Vickers indenter and one kilogram load. Indents were made on the (001) plane with the diagonals of the indenter along the $\langle 110 \rangle$ directions in one case and the $\langle 100 \rangle$ directions in another. Microhardness was also measured on the (110) plane, in this case with the diagonals of the indenter along the $[\bar{1}10]$ and $[001]$ directions. Five measurements were carried out for each orientation to obtain averages of the hardness (H) and the crack length (c). Indentation fracture toughness was calculated using these average values and the equation reported in [7]:

$$K = 0.016 \left(\frac{E}{H} \right)^{1/2} \left(\frac{P}{c^{3/2}} \right) \quad (1)$$

where E was taken as the Young's modulus of the single crystal along the indentation direction and P is the load (1 kg). Micrographs of the indents were taken in an optical microscope equipped to obtain Nomarski contrast and also in a JEOL 6300FXV Scanning Electron Microscope (SEM).

3. Results

3.1 Hardness and Fracture Toughness

The values of hardness and indentation toughness measured on the three orientations depended on the crystallography and the presence of Al (Fig. 1).

Note that the trend of the hardness with orientation is the same for both alloys, i.e., $H_{(001)\langle 110 \rangle} > H_{(110)[\bar{1}10]/[001]} > H_{(001)\langle 100 \rangle}$. The Al alloying produced a uniform reduction of the hardness of approximately 25% with respect to pure MoSi_2 for all orientations. This reduction is significantly larger than the error bars and is consistent but smaller than that reported for polycrystalline material [4]. The approximate values of the fracture toughness (Fig. 1b) were calculated for each orientation using Eq. (1). Note that there is a clear trend as a function of orientation, i.e., $K_{(001)\langle 110 \rangle} > K_{(001)\langle 100 \rangle} > K_{(110)[\bar{1}10]/[001]}$. The presence of Al seemed to increase the toughness in all cases. The results of Fig. 1b also show that the largest increase in toughness with respect to pure MoSi_2 , approximately 27%, occurred for indents with the $(001)\langle 110 \rangle$ orientation. However, the differences between pure MoSi_2 and $\text{Mo}(\text{Si},\text{Al})_2$ were within the order of magnitude of the error bars for all cases.

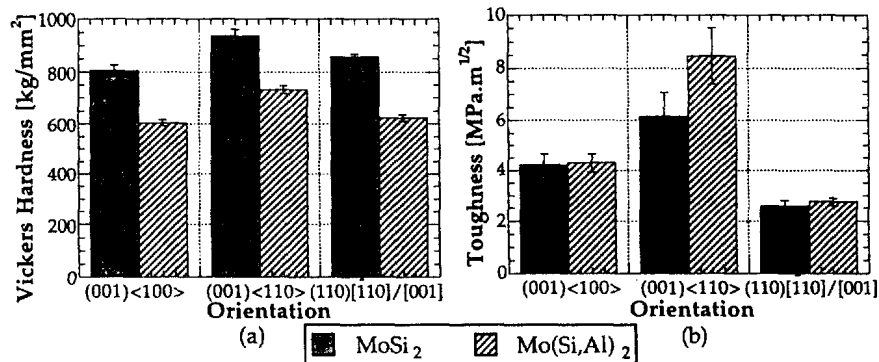


Figure 1. Vickers hardness (a) and indentation fracture toughness (b) for the two alloys as a function of orientation.

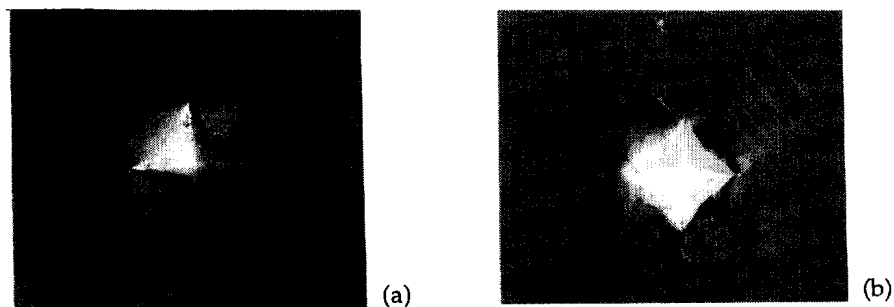


Figure 2. Indents on the (001) plane with diagonals along $\langle 110 \rangle$ directions. (a) $\text{Mo}(\text{Si},\text{Al})_2$; (b) MoSi_2 .

3.2. Slip and Cracking Behavior

3.2.1. Indents on the (001) Plane. Optical micrographs of the indents made on (001) with diagonals along $\langle 110 \rangle$ directions (Fig. 2) for both $\text{Mo}(\text{Si},\text{Al})_2$ and MoSi_2 reveal a significant difference between the slip traces present in each material. The slip lines observed in $\text{Mo}(\text{Si},\text{Al})_2$ (Fig. 2a) ran along the $\langle 110 \rangle$ directions, whereas the slip traces observed in MoSi_2 (Fig. 2b) were parallel to the $\langle 100 \rangle$ directions.

The corresponding SEM images (Fig. 3) show cracks (initially along $\langle 110 \rangle$) "splitting" or directly propagating along the $\langle 100 \rangle$ directions in both materials. Pure MoSi_2 had a higher density of cracks than the $\text{Mo}(\text{Si},\text{Al})_2$ sample (Fig. 3). The curvature of the indentation edges was more pronounced for $\text{Mo}(\text{Si},\text{Al})_2$, which was not observed when the diagonals of the indenter were along $\langle 100 \rangle$ directions (Fig. 4). No obvious slip lines were observed in the sample alloyed with Al for this orientation (Fig. 4a). Pure MoSi_2 (Fig. 4b), on the other hand, had slip lines parallel to $\langle 100 \rangle$, similar to those showed in Fig. 1b. In both samples the cracks emanated straight, without branching, from the corners of the indents (Fig. 5), and they had approximately the same length for all four corners of the indent.

3.2.2. Indents on the (110) Plane. The crack geometry was different for the indents made on the (110) plane (Fig. 6). Slip lines could not be resolved for the $\text{Mo}(\text{Si},\text{Al})_2$ sample in this case either, whereas a few faint slip lines could be observed in the MoSi_2 sample, running at approximately 60° from the $[\bar{1}10]$ direction. The thick vertical lines to the left of the indent in Fig. 6b are polishing scratches.

The crack behavior was highly anisotropic, since the $\text{Mo}(\text{Si},\text{Al})_2$ sample had long cracks running along the trace of the (001) plane, and short cracks corresponding to the diagonal parallel to the [001]

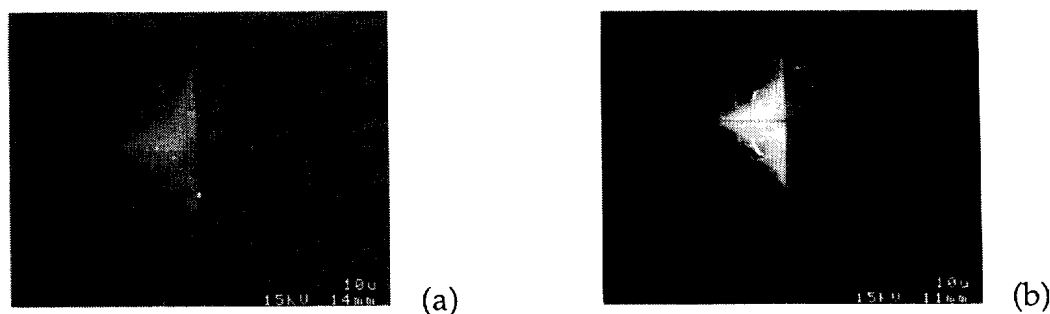


Figure 3. SEM images of the indents on the (001) plane with diagonals along $\langle 110 \rangle$ directions. (a) $\text{Mo}(\text{Si},\text{Al})_2$; (b) MoSi_2 .

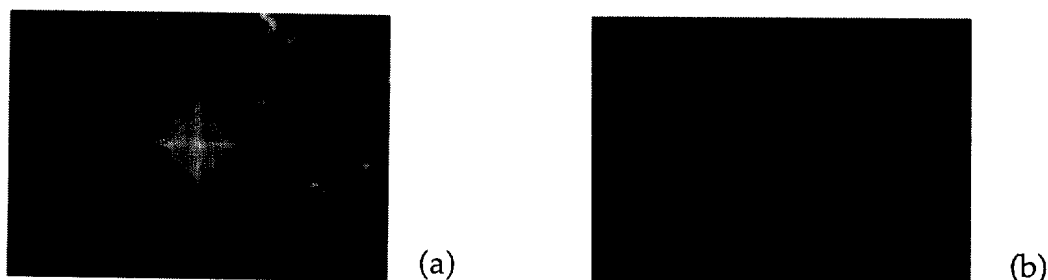


Figure 4. Indents on the (001) plane with diagonals along $\langle 100 \rangle$ directions. (a) $\text{Mo}(\text{Si},\text{Al})_2$; (b) MoSi_2 .

direction. Note that these cracks did not originate at the corners of the indent. Something similar occurred in MoSi_2 , except that in this case there was branching of the cracks running along $[\bar{1}10]$.

4. Discussion

The reduction in hardness in $\text{Mo}(\text{Si},\text{Al})_2$ was probably due to enhanced plasticity, as evidenced by the slip patterns presented in Fig. 2. The pincushion shape of the indent observed in $\text{Mo}(\text{Si},\text{Al})_2$ for that orientation is evidence of material sinking in around the indenter, which is typical in annealed metals [8], suggesting that $\langle 110 \rangle$ directions are "soft". The same was observed in pure MoSi_2 (Fig. 2b) but to a lesser degree, which also agrees with the relative values of the hardness. The piling up of material, observed around the indents in Fig. 3, occurs in work-hardened materials [8,9] indicating a high work hardening in the $\langle 100 \rangle$ directions. The difficulties to resolve slip for the (001) $\langle 100 \rangle$ and (110)[110]/[001] orientations in the Al-alloyed material could result from the presence of slip steps too small to be resolved by the technique used, as well as the possibility of having slip systems with Burgers vectors that do not produce adequate slip steps at the surface. These all indicate strong changes in the dislocation plasticity due to the presence of Al. The differences in slip behavior observed for the (001) $\langle 110 \rangle$ orientation indicate that the presence of Al affected the values of the Critical Resolved Shear Stresses (CRSS) for a set of slip systems. For pure MoSi_2 , the traces observed can result from slip on $\{023\}$, $\{013\}$, $\{010\}$, or $\{011\}$ planes, all of which have been reported [10,11]. $\{013\}1/2\langle 331 \rangle$ and $\{011\}\langle 100 \rangle$ are the most likely slip systems to be active, as they are the only systems involving the aforementioned planes that have been reported at room temperature [11]. The traces observed in the sample alloyed with Al are consistent with slip on $\{110\}1/2\langle 111 \rangle$, which has not been observed to be active at room temperature in pure MoSi_2 [11]. The slip traces observed in pure MoSi_2 for the

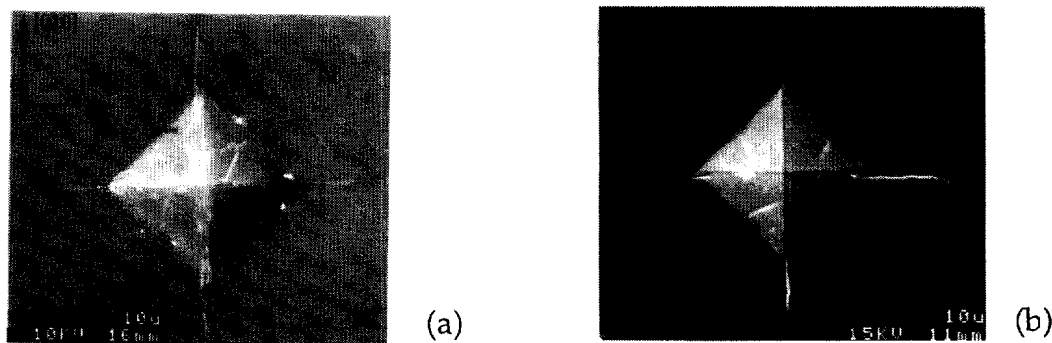


Figure 5. SEM images of the indents on the (001) plane with diagonals along $\langle 100 \rangle$ directions. (a) $\text{Mo}(\text{Si},\text{Al})_2$; (b) MoSi_2 .



Figure 6. Indents on the (110) plane with diagonals along $\bar{1}10$ and [001] directions. (a) $\text{Mo}(\text{Si},\text{Al})_2$; (b) MoSi_2 .

(110)[$\bar{1}10$]/[001] orientation correspond only to the $\{011\}$ planes, since the traces of $\{013\}$ planes on the (110) face would be at an angle of 30° with the [$\bar{1}10$] direction, instead of 60° . These facts suggest that the presence of Al reduced the CRSS of the $\{110\}1/2<111>$ systems such that they are favored over slip by $\{013\}1/2<331>$ or $\{011\}<100>$ at room temperature. Preliminary work on the effect of Al on the lattice parameters and the elastic constants of C11_b MoSi_2 [12], suggests that Al reduces the Peierls stress, which agrees with the observed reduction in hardness and the changes in the slip patterns.

The differences in the cracking behavior for the three orientations tested suggest that (001) and $\{100\}$ planes are preferred for cleavage in both alloys, evidenced by the long straight cracks observed along directions parallel to the traces of those planes. The values of the fracture toughness shown in Fig. 1b should be taken as qualitative only, since Eq. (1) was deduced for isotropic materials and in some cases the cracking was not limited to flaws growing from the corners (Fig. 2b) or the fracture behavior was anisotropic (Fig. 6). Nevertheless, the trend depicted by the values obtained indicates that the most favorable plane for cleavage should be the (001) followed by $\{100\}$ planes, whereas fracture on $\{110\}$ planes is not as favorable, as shown in Fig. 3. The differences in toughness between pure and Al alloyed MoSi_2 are probably too low to be significant except for the (001)<110> orientation. A more reliable method has to be used to measure the toughness.

The lateral cracks observed in pure MoSi_2 for the (110)[$\bar{1}10$]/[001] orientation could be related to particles of Mo_5Si_3 , which were detected in the SEM using Energy Dispersion Spectroscopy. The branching could be the result of cracks between particles, which align themselves along <110> directions in the MoSi_2 matrix [13].

5. Conclusions

- 1.- The solid solution addition of Al substituting for Si in C11_b MoSi_2 single crystals produces a well defined change in the slip around a Vickers indent. The slip traces for indentation in the (001)<110> orientation are consistent with slip planes, $\{110\}$, that had not been observed to be active in pure MoSi_2 tested in uniaxial compression at room temperature, indicating that Al significantly lowers the CRSS for slip on the $\{110\}1/2<111>$ systems. The lack of detectable slip traces in the alloyed material for the (001)<100> and (110)[$\bar{1}10$]/[001] orientations, as compared to pure MoSi_2 , gives further evidence that Al significantly changes the dislocation plasticity.
- 2.- The Vickers hardness of C11_b $\text{Mo}(\text{Si},\text{Al})_2$ is significantly lower than that of pure MoSi_2 for the range of orientations studied, which can be attributed to changes in the plastic behavior due to the presence of Al. The indentation toughness, however, is only slightly higher in general, and the differences are not likely to be significant. More work is needed to quantify the difference between the fracture toughness of these two materials reliably.

- 3.- The changes in crack geometry as a function of the orientation of the indent suggest that the preferred cleavage plane for both MoSi_2 and $\text{Mo}(\text{Si},\text{Al})_2$ is (001), followed by the {100} planes, whereas the {110} planes are not favorable for cleavage.

Acknowledgments

This work was supported by the US Department of Energy, Office of Basic Energy Science, and a Director Funded Postdoctoral Fellowship at LANL.

References

1. J.J. Petrovic, *Mat. Sci. Eng.*, A192/193, 31 (1995).
2. K. Yanagihara, K. Przybylski, and T. Maruyama, *Oxid. Metals*, **47**, 277 (1997).
3. Y. Suzuki, T. Sekino, and K. Niihara, *Scripta metall. mater.*, **33**, 69 (1995).
4. A. Costa e Silva and M.J. Kaufman, *Scripta metall. mater.*, **29**, 1141 (1993).
5. D.M. Shah, D. Berczik, D.L. Anton, and R. Hecht, *Mat. Sci. Eng.*, A155, 45 (1992).
6. H. Inui, M. Moriwaki, K. Ito, and M. Yamaguchi, to appear in *Phil. Mag. A*, 1997.
7. G.R. Anstis, P. Chantikul, B.R. Lawn, and D.B. Marshall, *J. Am. Ceram. Soc.*, **64**, 533 (1981).
8. American Society for Metals, "Hardness Testing", H.E. Boyer ed., ASM International, Metals Park, OH (1987).
9. R. Hill, B. Storåkers, and A.B. Zdunek, *Proc. R. Soc. Lond. A*, **423**, 301 (1989).
10. S.A. Maloy, T.E. Mitchell and A.H. Hauer, *Acta metall. mater.*, **43**, 657 (1995).
11. K. Ito, H. Inui, Y. Shirai, and M. Yamaguchi, *Phil. Mag. A*, **72**, 1075 (1995).
12. F. Chu, *Private Communication*, 1997.
13. S.Q. Xiao, S.A. Maloy, A.H. Heuer, and U. Dahmen, *Phil. Mag. A*, **72**, 997 (1995).